Single-Enzyme Analysis

DOI: 10.1002/anie.201003604

A Versatile DNA Nanochip for Direct Analysis of DNA Base-Excision Repair**

Masayuki Endo, Yousuke Katsuda, Kumi Hidaka, and Hiroshi Sugiyama**

Direct observation of enzymes interacting with DNA should be one of the ultimate technologies for investigating the mechanical behavior of the enzymes during the reactions. Atomic force microscopy (AFM) enables observation of biomolecules at a nanoscale spatial resolution; however, for a stable analysis, a scaffold to observe the reaction should be explored. DNA origami has recently been developed for the construction of a wide variety of multidimensional nanostructures, which can be used as scaffolds to incorporate various functionalities at specific positions.[1,2] We intended to construct an AFM-based analysis system for DNA repair using a DNA origami scaffold carrying various substrate double-stranded DNAs (dsDNA). We employed DNA base-excision repair (BER) enzymes 8-oxoguanine glycosylase (hOgg1) and T4 pyrimidine dimer glycosylase (PDG) to analyze the reaction on the DNA scaffold (Figure 1 a).[3,4] In the repair process, hOgg1 removes 8-oxoguanine (oxoG) to prevent G:C→T:A transversion during replication by DNA glycosylase activity and endonuclease activity for apurine–apyrimidine (AP) sites (AP-lyase activity) (Figure 1 a).[3,5] PDG removes photodamaged pyrimidine dimer including *cis–syn* cyclobutane thymine dimer (T<>T) by DNA glycosylase/AP-lyase activity.[4,6] BER enzymes often require structural changes of the target DNA strands, such as DNA bending, for the reaction to proceed.[3,4] The enzyme hOgg1 bends double-helix DNA by about 70° with flipping out of the oxoG for procession of the excision.[5] The enzyme PDG bends double-helix DNA by 60° with flipping out of the 3′-side of A in the opposite strand of T<>T.[8,9] The glycosylase/AP-lyase activity of these enzymes leads to single-strand scission at the damaged nucleotide (Figure 1 b). In addition, the reaction intermediates of both reactions form a covalent bond with the enzyme by reduction with $NaBH_4$.[5,10] We recently developed a framelike DNA origami scaffold to incorporate two different substrate dsDNAs.[11] If the above-mentioned enzymatic and chemical reactions

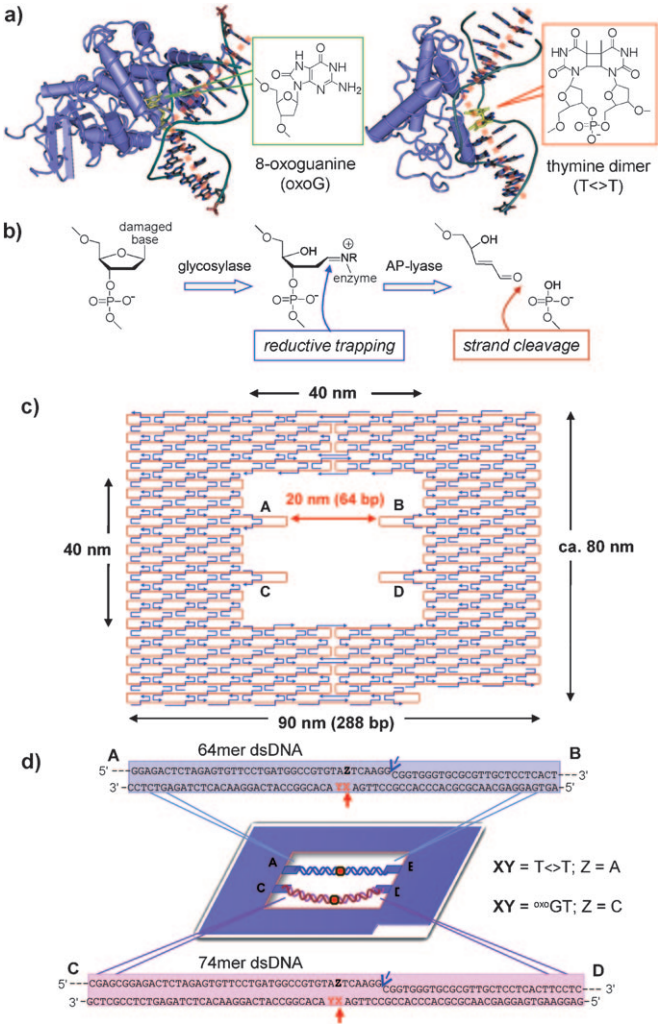

Figure 1. Analysis system for single DNA base-excision repair on a DNA nanochip. a) Crystal structure of hOgg1 (PDB: 1EBM) and T4 PDG (PDB: 1VAS) complexed with 8-oxoguanine- and thymine dimer-containing dsDNA, respectively. Orange dotted lines show bending of dsDNA. b) Scheme for the removal of a damaged base by glycosylase activity and single-strand DNA cleavage by AP-lyase activity. c) A designed DNA scaffold for a DNA nanochip. d) DNA nanochip carrying two dsDNAs and the sequences of the dsDNAs containing oxoG or T<>T at the center. Two dsDNAs, 64mer and 74mer, were placed onto the DNA scaffold. Cleavage sites are indicated by red arrow. A nick is introduced into the complementary strand (blue arrow)

[*] Dr. M. Endo, Prof. Dr. H. Sugiyama
Institute for Integrated Cell-Material Sciences (iCeMS)
Kyoto University
Yoshida-ushinomiyacho, Sakyo-ku, Kyoto 606-8501 (Japan)
Fax: (+81) 75-753-3670
E-mail: endo@kuchem.kyoto-u.ac.jp
hs@kuchem.kyoto-u.ac.jp
Y. Katsuda, K. Hidaka, Prof. Dr. H. Sugiyama
Department of Chemistry, Graduate School of Science
Kyoto University
Kitashirakawa-oiwakecho, Sakyo-ku, Kyoto 606-8502 (Japan)
Dr. M. Endo, Prof. Dr. H. Sugiyama
Japan Science and Technology Corporation (JST)
Sanbancho, Chiyoda-ku, Tokyo 102-0075 (Japan)

[**] This work was supported by Core Research for Evolutional Science and Technology (CREST) of JST, and a grant-in-aid of MEXT (Japan)
Supporting information for this article is available on the WWW under http://dx.doi.org/10.1002/anie.201003604.

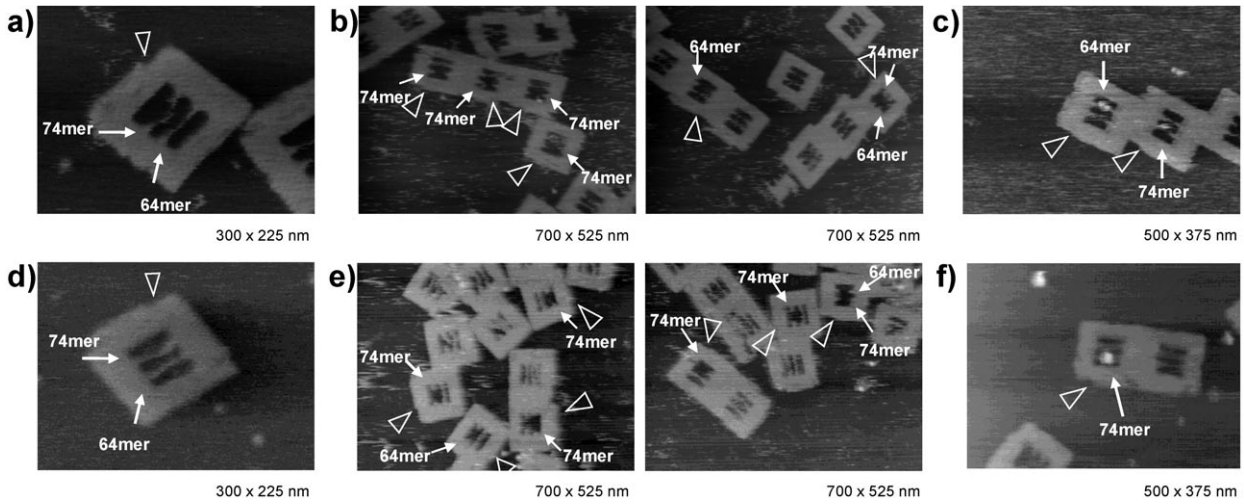

Figure 2. AFM images of DNA nanochips carrying two different duplexes and the reactions with hOgg1 and PDG. a) DNA nanochips carrying two different lengths of duplexes containing oxoG. b) Cleavage of dsDNA on the nanochip after the reaction with hOgg1. c) hOgg1 trapped by $NaBH_4$ reduction. d) DNA nanochips carrying two different lengths of duplexes containing T<>T. e) Cleavage of dsDNA on the nanochip after the reaction with PDG. f) PDG trapped by $NaBH_4$ reduction. The 64mer and 74mer strands can be identified by the lack of the right bottom corner (orientation marker; white triangle).

characteristic for the BER enzymes can be visualized in the defined DNA nanostructures, the behavior of the BER enzymes involved in the reactions can be analyzed at a single-molecular level.

For these purposes, we designed a 2D DNA scaffold with a vacant area inside. We placed various dsDNAs having a damaged nucleobase onto a defined DNA nanostructure as a dsDNA cassette, which we call a "DNA nanochip", and analyzed the DNA-repair reaction (Figure 1c). We installed the following four options for the analysis of the enzymes on the DNA nanochips: 1) placement of two different lengths of the substrate dsDNAs, tensed and relaxed dsDNAs, on a DNA nanochip to observe the structural effect on the reactions; 2) introduction of a nick in the opposite strand to observe the double-strand break after single-strand scission by glycosylase/AP-lyase activity; 3) detection of covalent-bond formation of the intermediates of the reaction with enzymes by $NaBH_4$ reduction; 4) visualization of the movement of the enzymes on the substrate dsDNAs on the DNA nanochip.

We introduced a tensed 64mer dsDNA and a relaxed 74mer dsDNA onto the DNA nanochip, which contain oxoG or T<>T at the center of the dsDNAs (Figure 1c). The 64mer dsDNA just fitted as a tensed strand in the cavity, while the 74mer strand is a more relaxed duplex that can allow bending of the dsDNA by at least 60° at a damaged nucleoside located at the center (Figure S1 in the Supporting Information). Using these DNA nanochips, we observed cleavage of the DNA strand and reductive trapping of the intermediate, and analyzed the effect of DNA tensions on these reactions. In addition, dynamic movement of the enzymes and the single DNA-repair reaction were directly observed using a fast-scanning AFM imaging system, and the trajectory of the enzymes on the DNA nanochip was analyzed.

The DNA nanostructure was designed using a reported DNA origami method.[1] M13mp18 single-stranded DNA and complementary DNA strands (staple strands) were annealed in a solution containing Tris-HCl buffer (pH 7.6; Tris = tris(hydroxymethyl)aminomethane), ethylenediaminetetraacetic acid (EDTA), and Mg^{2+} from 85 °C to 15 °C at a rate of $-1.0\,^{\circ}C\,min^{-1}$. For introduction of the dsDNAs into the DNA nanochip, synthetic 64mer and 74mer dsDNAs were introduced between the connection sites A–B and C–D, respectively (Figure 1d), by annealing from 40 °C to 15 °C at a rate of $-1.0\,^{\circ}C\,min^{-1}$. In the complementary strands, a nick was introduced for the subsequent double-strand cleavage after single-strand cleavage at the oxoG or T<>T site (Figure 1d). AFM images were obtained in the same buffer solution, and different tensions of the two dsDNAs containing oxoG and T<>T were observed on the nanochips (Figure 2a and d, respectively). Using fast-scanning AFM imaging, which can successively acquire one AFM image per second,[12] movement of the 74mer dsDNA was observed on the DNA nanochip, whereas movement of the 64mer dsDNA was modest, which is similar to the previous case.[11]

The glycosylase/AP-lyase activity of hOgg1 was observed on the DNA nanochip. Double-strand cleavage of the tensed 64mer and 74mer dsDNAs was performed by treatment with hOgg1 and was observed by AFM (Figure 2b and Figure S2a). After treatment with hOgg1, 32% of the 74mer dsDNA and 11% of the 64mer dsDNA were cleaved, and the other nanochips (57%) left uncleaved. The results also show that the oxoG in the relaxed 74mer dsDNA is a better substrate for hOgg1 than that in the tensed 64mer dsDNA. We introduced the unmodified 74mer dsDNAs having guanine instead of oxoG to confirm the substrate specificity. When the nanochip was treated with hOgg1, the unmodified dsDNA left uncleaved, indicating that this observation system worked only for the oxoG substrate.

We examined the formation of a covalent linkage between a reaction intermediate and hOgg1 using a reducing agent ($NaBH_4$ trapping assay). During the glycosylation and

subsequent reaction, BER enzymes covalently bind to the C1′ site of ribose through an amino nucleophile to eliminate a damaged nucleobase and form a Schiff base intermediate, which can be reduced by hydrogenation with $NaBH_4$ to form a stable covalent linkage between opened ribose and enzyme.[5] After reaction in the presence of $NaBH_4$, hOgg1 that was attached to the center of the dsDNA was observed on the DNA nanochip, which did not move further during AFM scanning (Figure 2c and Figure S3a). This result indicates that the intermediate in the repair process was covalently trapped even in the designed nanospace. The yields of the trapped hOgg1 for the 64mer and 74mer dsDNAs were 8% and 27%, respectively, which are comparable with the results of the cleavage of the 64mer and 74mer dsDNAs (Table 1).

Table 1: Direct observation of double-strand cleavage and $NaBH_4$ trapping on the DNA nanochip. The reactions were carried out in solution, and then the number of events was observed by AFM.

		hOgg1		PDG	
		64 mer dsDNA	74 mer dsDNA	64 mer dsDNA	74 mer dsDNA
double-strand cleavage	number of events	14 (11%)	41 (32%)	9 (7%)	28 (29%)
	total nanochips	129		187	
$NaBH_4$ trapping assay	number of events	23 (8%)	80 (27%)	13 (13%)	37 (37%)
	total nanochips	292		100	

Glycosylase/AP-lyase activity of hOgg1 can be detected using the DNA nanochip system. In the previous AFM study of hOgg1–dsDNA complex formation, hOgg1 bends the dsDNA by about 71°.[13] In our nanochip system, the 74mer dsDNA bends at least 60° (Figure S1). As shown in the cleavage and reductive trapping assays, the binding to the relaxed 74mer preferentially occurred as compared with the tensed 64mer dsDNA.

We next examined the glycosylase/AP-lyase activity of PDG by direct observation of the cleavage of 64mer and 74mer T<>T-containing dsDNAs on the DNA nanochip. AFM images were obtained after the reaction of PDG with substrate dsDNAs (Figure 2e and Figure S2b). After treatment with PDG, 29% of 74mer dsDNA and 7% of 64mer dsDNA were cleaved. The results show that the 74mer dsDNA was more effectively cleaved than the 64mer dsDNA. We also introduced unmodified DNA strands having two thymidines instead of T<>T onto the DNA nanochip. PDG did not cleave the unmodified DNA strand, meaning that this nanochip system also selectively worked for the T<>T substrate.

We also examined the covalent attachment of PDG trapped on the T<>T site on the DNA nanochip by reductive $NaBH_4$ trapping assay.[8] In the presence of $NaBH_4$, PDG that was covalently bound to the center of the dsDNA was observed (Figure 2f). The results also showed that the intermediate of the PDG repair process was trapped on the DNA nanochip. The yields of the trapped PDG for a tensed 64mer and a relaxed 74mer dsDNA substrate were 13% and 37%, respectively, which was also comparable with the results of the cleavage of the 64mer and 74mer dsDNAs (Table 1). These results show that the glycosylase/AP-lyase activity of single BER enzymes can be precisely monitored using the DNA nanochip system.

Bending of the dsDNA for glycosylation is required for the reaction to proceed. The relaxed strand can accommodate hOgg1 and PDG to bind and bend the target sequence. In contrast, the tensed strand allows binding of these enzymes, whereas this strand is a poor substrate for bending, resulting in the poor DNA cleavage and reductive trapping.

We next tried to observe directly the cleavage reaction of hOgg1 on the DNA nanochip using a fast-scanning AFM imaging system (Figure 3, Movie S1 in the Supporting Information). Successive images were acquired every 1 s. We observed single hOgg1 attached to the center of the 74mer dsDNA, and hOgg1 bound to the 74mer dsDNA did not dissociate from the dsDNA during the observation for more than 30 s. This result shows that binding of hOgg1 to the dsDNA was stable enough to observe the behavior of hOgg1 on the nanochip. In the successive images, hOgg1 rapidly

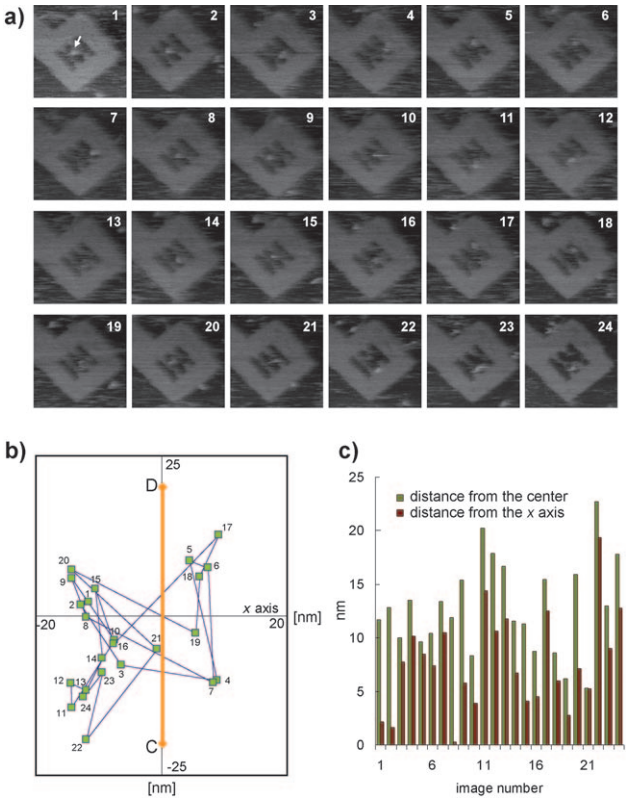

Figure 3. Fast-scanning AFM images of the movement and reaction of hOgg1. a) Successive AFM images were obtained every 1 s. Image size 200×200 nm. The image number corresponds to the lapsed time. b) Trajectory of the movement of hOgg1 bound to 74mer dsDNA on the nanochip. C and D represent the positions of connectors C and D in the nanochip. c) hOgg1 position on the DNA nanochip; distance from the center of the trajectory graph and from the horizontal axis (*x* axis) of the 74mer dsDNA.

moved on the 74mer dsDNA, searching oxoG for catalyzing the reaction. At a time of 22 s, the dsDNA was cleaved, and hOgg1 did not move further, attaching to the end of the cleaved dsDNA.

The positions of hOgg1 binding to the 74mer dsDNA are shown as a trajectory (Figure 3b and Figure S4), where the number corresponds to the image number. The distances between the hOgg1 and the center of the connection sites C and D for bridging 74mer dsDNA are summarized in Figure 3c. Because the oxoG was introduced to the center of the 74mer dsDNA, the position of the oxoG should be close to the center of the connection sites C and D and the horizontal axis (x-axis) during the movement. So the catalytic reaction at the oxoG should occur when the hOgg1 was located close to the center. When the positions of hOgg1 are far from the oxoG (for example, images 11, 17, and 20), the catalytic reaction could hardly occur. The position of hOgg1 in image 21, which was 1 s before the double-strand breakage (image 22), is close to the center (oxoG) of the 74mer dsDNA, so the cleavage reaction should occur at this moment. By using this analysis, although we did not clearly identify the time period when the glycosylase/AP-lyase reaction proceeded, we were able to observe directly the cleavage reaction over this time range.

We next observed a series of PDG reactions on the DNA nanochip: binding to the substrate dsDNA, catalyzing the reaction, cleavage of the DNA strand, and dissociation from the cleaved dsDNA by a fast-scanning AFM imaging system (Figure 4, Movie S2).[14] The successive AFM images were acquired every 5 s. In a series of reactions, at first, single PDG attached to the end of the 74mer dsDNA in the DNA nanochip, and the PDG stayed without moving. After 15 s, the PDG slid on the 74mer dsDNA, then in the next image (time 20 s), cleavage of the 74mer dsDNA was observed (Figure 4a). The PDG stayed at the end of the cleaved strand (times 20–50 s), and then dissociated along the cleaved DNA strand (times 55 s and 60 s) (Figure 4b). PDG sliding on the dsDNA was observed during a period of 15 s before cleavage; therefore, we identified the time period of the glycosylase/AP-lyase reaction of PDG by direct observation using a fast-scanning AFM imaging system.

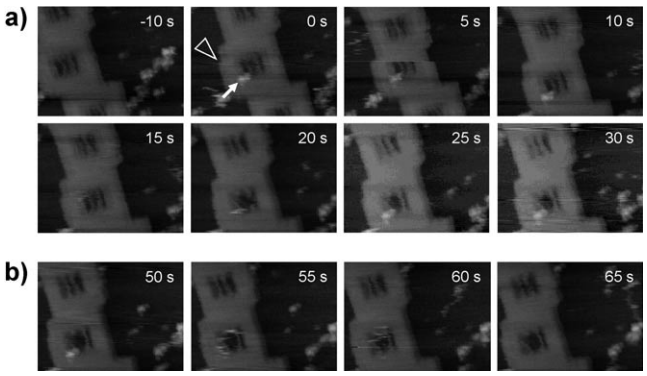

Figure 4. Fast-scanning AFM images of the reaction events with PDG. a) Successive AFM images of PDG binding to the 74mer dsDNA and dsDNA cleavage. b) Successive AFM images of dissociation of PDG from the cleaved dsDNA. AFM images were obtained every 5 s. Image size 300×225 nm.

We found that the enzymes sometimes attach to the scaffold DNA. However, they easily detached during AFM scanning because of the close packing of the DNAs in the origami scaffold. Thus, the enzymes preferentially recognize and bind to the incorporated dsDNAs on the nanochip.

In conclusion, we have created tension-controlled dsDNA substrates in a DNA nanoscale scaffold and shown the importance of DNA-strand relaxation in allowing double-helix bending during the glycosylation/AP-lyation reaction of hOgg1 and PDG. The DNA nanochip can be a versatile scaffold to observe single-molecular behavior of DNA-binding enzymes. In addition, the DNA nanochip is valuable for analyzing the motion of the enzyme because of its defined coordinated space. The exact position and displacement of the enzyme in the reaction on the dsDNA can be monitored and analyzed. Therefore, the time-resolved reaction coordination between the enzymes and substrate can be estimated at nanoscale spatial resolution. For analysis of the enzymes on the DNA nanochips, various options can be installed, such as incorporation of various nucleoside analogues, placement of various lengths of dsDNAs, and detection of DNA cleavage and covalent binding of the enzymes to the dsDNA. In this nanochip system, these DNA substrates can be easily incorporated as a cassette of dsDNA, depending on the research purpose. The method could be extended to the direct observation and analysis of various enzymatic phenomena in the designed nanoscale spaces.

Experimental Section

DNA nanochip formation and introduction of substrate dsDNAs: The DNA nanostructure was assembled in a 20 μL solution containing M13mp18 single-stranded DNA (New England Biolabs; 10 nM), staple strands (226 strands; 50 nM; 5 equiv), 20 mM Tris buffer (pH 7.6), 1 mM EDTA, and 10 mM $MgCl_2$.[11] The mixture was annealed from 85 °C to 15 °C at a rate of $-1.0\,°C\,min^{-1}$. The 8-oxoguanine- and thymine dimer-containing DNA strands were prepared using an automated DNA synthesizer using 8-oxoguanine and thymine dimer phosphoramidites (Glen Research) and purified by denaturing PAGE. Duplexes were prepared by annealing the corresponding DNA strands, and duplex strands (five equivalent excess) were incorporated into the DNA nanochip by heating at 40 °C and then cooling to 15 °C at a rate of $-1.0\,°C\,min^{-1}$ using a thermal cycler.

Cleavage of substrate dsDNAs on the DNA nanochips with PDG and hOgg1: A DNA nanochip containing both 64 mer and 74 mer substrate dsDNAs was purified by electrophoresis using a 1% agarose gel, and the corresponding band was cut and recovered using a Freeze 'N Squeeze DNA gel extraction column (BioRad) by following the protocol. The reaction with hOgg1 was performed in a 10 μL solution containing purified DNA nanochip bearing two dsDNA substrates, hOgg1 (New England Biolabs), 50 mM Tris-HCl (pH 7.5), 50 mM NaCl, 10 mM $MgCl_2$, and 1 mM 1,4-dithiothreitol (DTT) at 37 °C for 1.5 h. The reaction with PDG was performed in a 10 μL solution containing purified DNA nanochip with two dsDNA substrates, T4 PDG (New England Biolabs), 50 mM Tris-HCl (pH 7.5), 100 mM NaCl, 10 mM $MgCl_2$, and 1 mM DTT at 37 °C for 1.5 h.

$NaBH_4$ trapping assay of reaction intermediates treated with hOgg1 and PDG: A purified DNA nanochip containing both 64 mer and 74 mer substrate dsDNAs was treated with hOgg1 or PDG in a 10 μL solution containing 50 mM Tris-HCl (pH 7.5), 50 mM $NaBH_4$, 1 mM EDTA, and 10 mM $MgCl_2$ at room temperature for 1 h.

Fast-scanning AFM imaging of the DNA nanochip: AFM images were obtained on a fast-scanning AFM system (Nano Live Vision, RIBM, Tsukuba, Japan) using a silicon nitride cantilever (resonant frequency = 1.0–2.0 MHz, spring constant = 0.1–0.3 $N m^{-1}$, EBDTip radius < 15 nm, Olympus BL-AC10EGS-A2). The sample (2 μL) was adsorbed on a freshly cleaved mica plate for 5 min at room temperature, and then washed with the reaction buffer solution to remove unbound enzymes. Scanning was performed in the same buffer solution in tapping mode.

Received: June 13, 2010
Revised: August 16, 2010
Published online: November 4, 2010

Keywords: DNA damage · enzymes · nanostructures · scanning probe microscopy · single-molecule studies

[1] P. W. K. Rothemund, *Nature* **2006**, *440*, 297 – 302.
[2] M. Endo, H. Sugiyama, *ChemBioChem* **2009**, *10*, 2420 – 2443.
[3] S. S. David, V. L. O'Shea, S. Kundu, *Nature* **2007**, *447*, 941 – 950.
[4] D. G. Vassylyev, K. Morikawa, *Curr. Opin. Struct. Biol.* **1997**, *7*, 103 – 109.
[5] H. M. S. D. Nash, Bruner, O. D. Schärer, T. Kawate, T. A. Addona, E. Spooner, W. S. Lane, G. L. Verdine, *Curr. Biol.* **1996**, *6*, 968 – 980.
[6] M. L. Dodson, M. L. Michaels, R. S. Lloyd, *J. Biol. Chem.* **1994**, *269*, 32709 – 32712.
[7] G. L. Verdine, S. D. Bruner, D. P. G. Norman, *Nature* **2000**, *403*, 859 – 866.
[8] K. Morikawa, O. Matsumoto, M. Tsujimoto, K. Katayanagi, M. Ariyoshi, T. Doi, M. Ikehara, T. Inaoka, E. Ohtsuka, *Science* **1992**, *256*, 523 – 526.
[9] D. G. Vassylyev, T. Kashiwagi, Y. Mikami, M. Ariyoshi, S. Iwai, E. Ohtsuka, K. Morikawa, *Cell* **1995**, *83*, 773 – 782.
[10] M. L. Dodson, R. D. Schrock, R. S. Lloyd, *Biochemistry* **1993**, *32*, 8284 – 8290.
[11] M. Endo, Y. Katsuda, K. Hidaka, H. Sugiyama, *J. Am. Chem. Soc.* **2010**, *132*, 1592 – 1597..
[12] T. Ando, N. Kodera, E. Takai, D. Maruyama, K. Saito, A. Toda, *Proc. Natl. Acad. Sci. USA* **2001**, *98*, 12468 – 12472.
[13] L. Chen, K. A. Haushalter, C. M. Lieber, G. L. Verdine, *Chem. Biol.* **2002**, *9*, 345 – 350.
[14] S. E. Halford, J. F. Marko, *Nucleic Acids Res.* **2004**, *32*, 3040 – 3052.

